Available online at www.sciencedirect.com
ScienceDirect
Journal of the European Ceramic Society 27 (2007) 723–727
www.elsevier.com/locate/jeurceramsoc

Hydrothermal synthesis of nickel ferrite powders, their properties and sintering

Mirosław M. Bućko *, Krzysztof Haberko

AGH University of Science and Technology, Faculty of Materials Science and Ceramics, al. Mickiewicza 30, 30-059 Cracow, Poland

Available online 5 June 2006

Abstract

$NiFe_2O_4$ powders were synthesized by co-precipitation with ammonia solution using aqueous solution of $NiCl_2$ and $FeCl_3$ followed by hydrothermal treatment of the precipitate. It was found that crystallization in water led to nanometric in size and isometric in shape crystallites, whereas crystallization in sodium hydroxide solution results in particles of well defined walls. Generally, particles crystallized in water were smaller and their particle size distribution was narrower than those crystallized in NaOH solution. Behaviour of the powders under dry compaction and sintering strongly depended on the powder morphology. The powder crystallized in NaOH solution gave compacts of higher density and sintered density of this powder was also higher than that of the powder processed in water.

Keywords: Powders-chemical preparation; Hydrothermal synthesis; Ferrites

1. Introduction

Many ferrites with the spinel structure, $MeFe_2O_4$ (where Me: Ni, Zn, Mn, Co, Cd or their mixtures), are extensively used in a number of electronic devices. This is because of its high permeability at high frequencies, remarkably high electrical resistivity, mechanical hardness, chemical stability and reasonably low cost.[1] They find applications in the wide range of frequencies and from low to high permeability. Since the last decade, quite new and interesting magnetic properties have been reported for nanocrystalline spinel ferrites. Large magnetic moments[2] and ferromagnetic or ferrimagnetic ordering[3] on grain size reduction to a few nanometers was observed. Colloidal magnetic materials have attracted a great deal of attention for technological application and fundamental studies. These involve biology, electronics, transport and information technology,[4] such as high-density data storage devices,[5] ferrofluids,[6] magnetic resonance imaging (as contrast agents), and magnetic refrigeration.[4] Moreover, nanometric ferrites are considered as important catalysts for CO_2 and H_2O decomposition[7] and gas sensors for gases like liquefied petroleum gas, ethanol, CO and CH_4.[8]

Much work on ferrites was carried out on microcrystalline ceramics prepared by the standard ceramic technique, involving high-temperature reactions between finely milled oxide (or carbonate) powders followed by shaping and successive pressing and sintering.[9] Such method does not allow controlling fully crystallite size and shape as well as powder properties. The spinel ferrites have also been successfully synthesized by other type of solid state reaction such as high-temperature self-propagating synthesis,[10] combustion synthesis,[11] and thermal decomposition of citrate[12] or polyethylene glycol precursor.[13] Recently, many publications have reported various preparation techniques based on wet-chemical reactions to obtain ferrite nanopowders. The most popular are: sol–gel methods,[14] microemulsion,[15] hydrothermal-microwave[16] and hydrothermal synthesis.[17–22] Among these methods, hydrothermal synthesis has attracted great interest because it is a promising route to produce highly crystallized, weakly agglomerated powders having a narrow size distribution. Several compositions were prepared by crystallization under hydrothermal conditions. Simple evidence is available to show that this process has some advantages in controlling particle size, morphology and other characteristics by adjusting reaction temperature, duration of the process, additives and other factors.[22,23]

Co-precipitated hydroxides or mixtures of separately prepared $Ni(OH)_2$ and FeO(OH) were used in hydrothermal synthesis of nickel ferrite.[18] The reaction was performed in of NaOH or ammonia solutions at different pH values as well as in pure water.[17,18] Resulting powders differed in sizes and shapes depending on the crystallization condition. Basing on

* Corresponding author. Tel.: +48 12 6172537; fax: +48 12 6334630.
E-mail address: bucko@uci.agh.edu.pl (M.M. Bućko).

0955-2219/$ – see front matter © 2006 Elsevier Ltd. All rights reserved.
doi:10.1016/j.jeurceramsoc.2006.04.052

the presented data, it can be concluded that the kinetics of ferrite formation as well as shape and size of its crystallites strongly depends on several factors such as the kind of precursor, pH value, temperature and duration of the hydrothermal process.

The aim of the present work was to study the hydrothermal synthesis of nickel ferrite powders, the shape of their crystallites, particle size distribution, compaction and sintering behaviour.

2. Experimental

Co-precipitation technique was applied to prepare a homogeneous mixture of Ni and Fe hydroxides. The starting aqueous solutions of $NiCl_2$ and $FeCl_3$ (∼1 M) were mixed in appropriate proportion and introduced drop wise into vigorously stirred sodium hydroxide solution (4 M). Volume proportion of both solutions was adjusted to give the final pH 12. The precipitated X-ray amorphous gel was washed with distilled water, until no reaction for chloride ions with $AgNO_3$ was detected. Excess of liquid phase was removed by vacuum filtration. The resulting gel was divided into two parts. One of them was mixed with 4 M NaOH solution and vacuum filtered again. Both gels were subjected to hydrothermal treatment at 240 °C for 8 h either in distilled water or in the NaOH solution. The sample crystallized in NaOH environment was washed with distilled water. The powders were dried at 60 °C for 24 h, ground in a mortar with oleic acid as lubricant and dried again at 130 °C overnight. Uniaxial pressing under 300 MPa allowed us to obtain green compacts of 12 mm diameter and about 3 mm height. The samples were sintered at 1200 °C for 1 h with 10 °C min^{-1} rate of temperature increase.

To estimate influence of the preparation conditions additional 2^k-type factorial experiment was performed using three selected factors. The first of them was the concentration of sodium hydroxide; its high level was established at 4 M and the low level at 0 (pure water). The two following factors were time and temperature of the hydrothermal treatment. Their levels were fixed at 8 and 2 h and 250 and 175 °C, respectively. Specific surface area of such powders was the controlling parameter.

X-ray diffraction using X'Pert Pro (Phillips PANalytical) was applied to identify phase composition of the powders and sintered materials. Observations under TEM (CM20, Philips) gave us information about morphology of the powders and their particle size distributions. Specific surface area (S) of the powders was determined by the nitrogen adsorption using the BET isotherm (Sorpty 1700, Carlo Erba). Equivalent particle sizes were calculated using the formula: $D_{BET} = 6(\rho S)^{-1}$, where $\rho = 5.368\ g\ cm^{-3}$ is the theoretical density of $NiFe_2O_4$. Apparent density of the green compacts was determined on the basis of their sizes and weight and that of the sintered materials by hydrostatic weighing. Relative densities were calculated using apparent densities and ρ.

3. Results and discussion

XRD analysis indicates that both powders as well as sintered materials are composed of nickel ferrite phase only. Most probably co-precipitation process results in a substance of extreme homogeneity. Fig. 1 shows TEM micrographs of the powders. The pictures illustrate essential influence of the hydrothermal crystallization environment on the size and shape of the nickel ferrite crystallites. Particles prepared in pure water are nanometric in their sizes and isometric in shape (marked H), contrary to those crystallized in NaOH solution (marked N). In the latter case hydrothermal crystallization resulted in particles of well defined

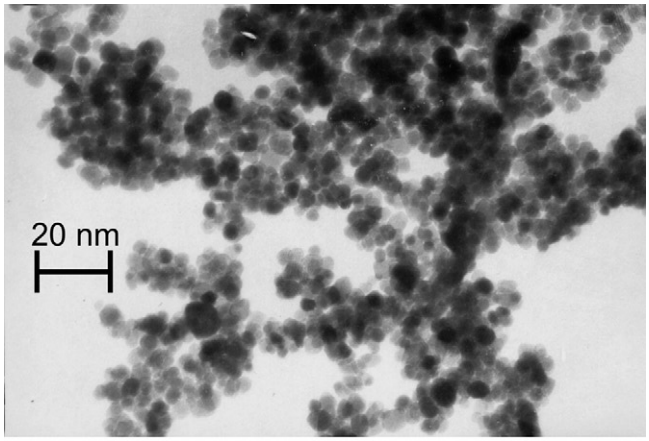

(a)

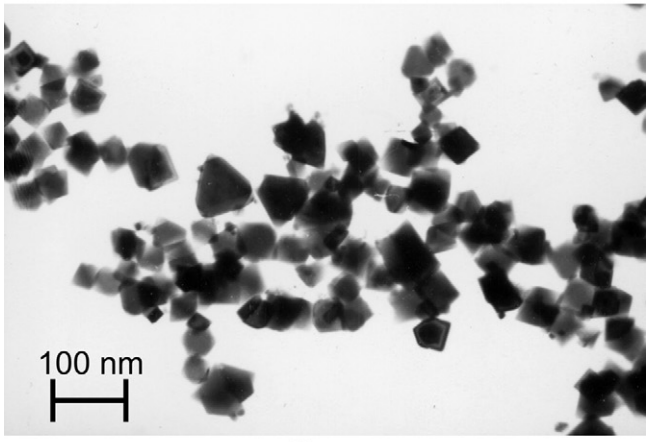

(b)

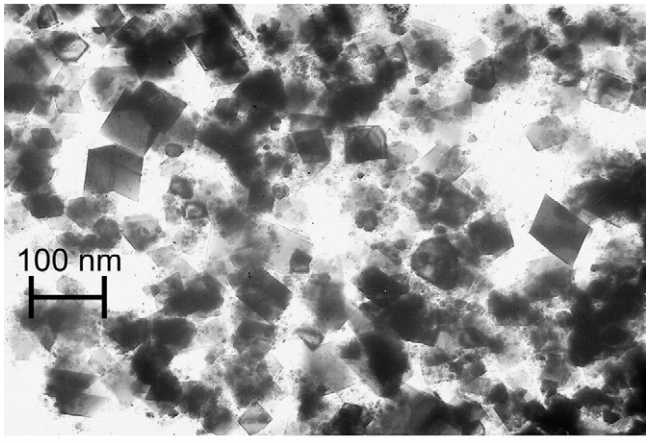

(c)

Fig. 1. TEM micrographs of the powders hydrothermally prepared in: (a) pure water, (b) 4 M NaOH solution, and (c) 2 M NaOH solution.

Table 1
The plan and the results of the factorial experiment

Experimental factors			Specific surface area ($m^2\ g^{-1}$)
NaOH concentration (M)	Time (h)	Temperature (°C)	
4	8	250	22.1
4	2	250	27.2
4	8	175	37.5
4	2	175	111.1
0	8	250	63.4
0	2	250	75.2
0	8	175	77.2
0	2	175	135.8
2	5	210	42.2

walls and micrometric sizes. Shapes of the particles crystallized under the basic conditions suggest that crystallite growth occurs in this case by the dissolution–precipitation process. This is corroborated by the morphology of the powder synthesized under conditions corresponding to the centre of the factorial experiment plan—2 M NaOH, 4 h, 210 °C (Fig. 1c).

Table 1 shows the plan of the factorial experiment and results that is specific surface area of the powders. Values of regression coefficients, b_i—only for the principal interactions, and corresponding t_i values are as follow:

$$b_1 = -19.21; \quad b_2 = -21.71; \quad b_3 = -18.64;$$

$$t_1 = 7.94; \quad t_2 = 8.97; \quad t_3 = 7.70$$

Because, the critical value of the t parameter for significance level $p = 0.05$ and degree of freedom $f = 2$ equals 4.39, it can be concluded that each of the investigated factors essentially influences particle size of nickel ferrite powders crystallized under hydrothermal condition.

Fig. 2 shows particle size distribution of the powders using the Rosin–Rammler coordinates. The powder crystallized in water (H) is much finer and shows much narrower particle size distribution than the one crystallized in NaOH solution (N). The latter feature is evidenced by the slope ratios indicated in Fig. 2. Mono-modal distribution occurs in the both powders. As it should be expected the powder H shows specific surface area $S = 83.5\ m^2\ g^{-1}$ and the powder N reveals $S = 25.3\ m^2\ g^{-1}$. These figures correspond to equivalent particle sizes $D_{BET} = 13.4$ nm and 44.1 nm, respectively.

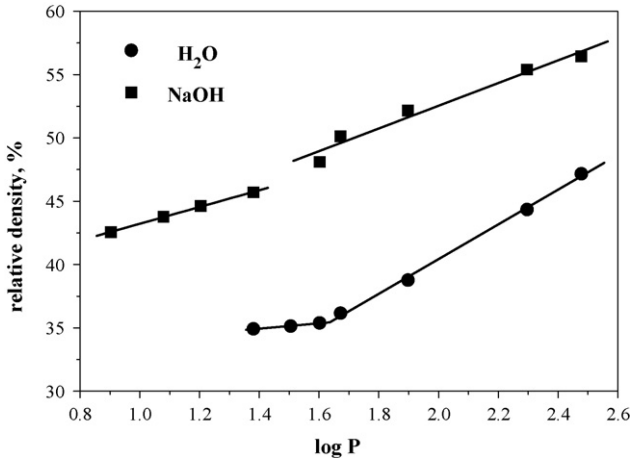

Fig. 3. Compaction diagrams. Crystallization environment indicated.

Fig. 3 shows relative densities of green bodies versus compaction pressure. In each case two straight line relationships in semi-logarithmic coordinates occurs. Such behaviour is characteristic of the powders composed of agglomerates. As it was shown in earlier studies,[24,25] at the pressure corresponding to the point of the segment intersection bonds within agglomerates break. Coarser powder (N) reaches higher densities than observed in the nanometric powder crystallized in water (H). The breaking point in case of the powder H falls in higher pressure. It indicates that agglomerates of this powder are stronger, which agrees with the Rumpf's[26] relation. According to this relation the agglomerate strength is inversely proportional to the particle size.

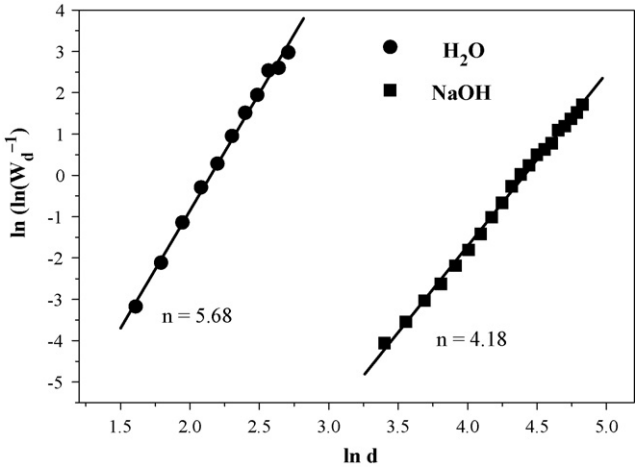

Fig. 2. The powder particle size distribution using Rosin–Rammler coordinates. Crystallization environment indicated. n, slope ratio.

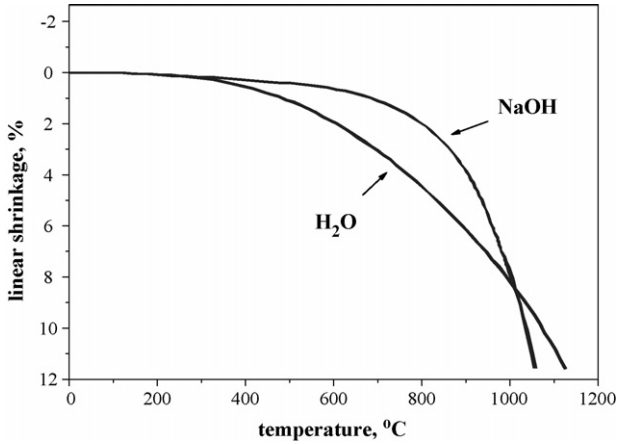

Fig. 4. Dilatometric curves. Rate of temperature increase 10 °C min^{-1}. Crystallization environment indicated.

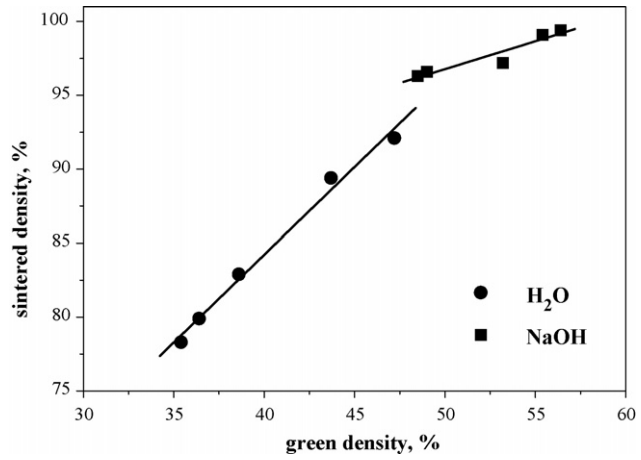

Fig. 5. Sintered density vs. green density of the powder compacts sintered at 1200 °C for 1 h. Crystallization environment indicated.

Compacts for sintering studies were uniaxially pressed under 300 MPa. Their relative densities are 48.1% and 56.8% for the finer (H) and coarser (N) powders, respectively. Fig. 4 shows linear shrinkage of the powder compacts. It can be notice that the nanometric powder (H) starts to shrink at lower temperature (at about 400 °C) whereas the beginning of sintering of the coarser one (N) corresponds to about 700 °C. We observe that the shrinkage line of the powder N is steeper than that for the powder H. Compacts of the former powder reach higher density at the same temperature of 1100 °C and 1 h soaking (95.9%) than the latter ones (90.5%). Such behaviour should most probably be attributed to the higher green density of the compacts made from the coarser powder. Further investigations corroborated the essential influence of the green density on the density of the sintered materials (Fig. 5). Nearly full densification (99.4%) is reached by the sample of the coarser powder (N) compacted under 300 MPa and sintered at 1200 °C for 1 h. Its microstructure is shown in Fig. 6.

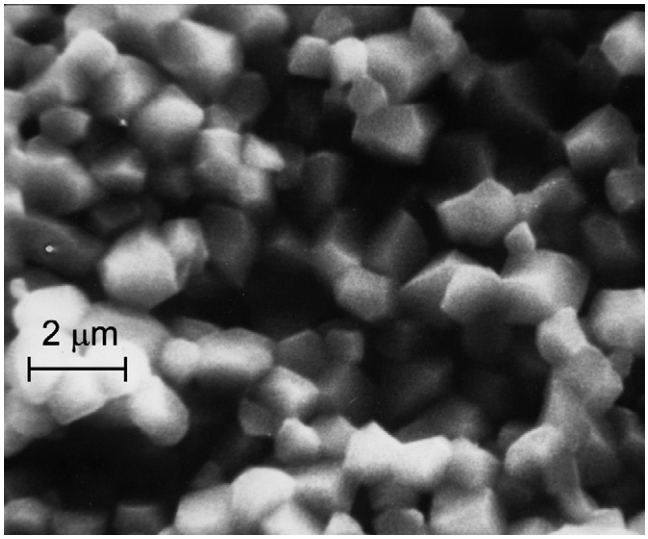

Fig. 6. Microstructure of the sample of the coarser powder (N) compacted under 300 MPa and sintered at 1200 °C for 1 h.

4. Summary

Co-precipitated nickel and iron X-ray amorphous gel subjected to the hydrothermal treatment result in crystallization of nickel ferrite particles. Morphology of the powder strongly depends on the crystallization environment. Particles of the powder crystallized in pure water are nearly spherical and nanometric in size and their particle size distribution is very narrow. However, those crystallized in NaOH solution are much coarser, show well defined walls and their size distribution is broader than in the case of the former ones. Morphological differences between the powders determine their behaviour during cold compaction and sintering. The coarser powder densifies better during dry compaction and sintering that the finer one. The powder crystallized in NaOH solution leads to the material of nearly full density and uniform microstructure.

References

1. Ishino, K. and Narumiya, Y., Development of magnetic ferrites: control and application of losses. *Ceram. Bull.*, 1987, **66**, 1469–1474.
2. Schiessl, W., Potzel, W., Karzel, H., Steiner, M., Kalvius, G. M., Martin, A. *et al.*, Magnetic properties of the $ZnFe_2O_4$ spinel. *Phys. Rev. B*, 1996, **53**, 9143–9152.
3. Burghart, F. J., Potzel, W., Kalvius, G. M., Schreier, E., Grosse, G., Noakes, D. R. *et al.*, Magnetism of crystalline and nanostructured $ZnFe_2O_4$. *Physica B*, 2000, **289–290**, 286–290.
4. Ziolo, R. F., Giannelis, E. P., Weinstein, B. A., O'Horo, M. P., Ganguli, B. N., Mehrotra, V. *et al.*, Matrix mediated synthesis of γ-Fe_2O_3: a new optically transparent magnetic material. *Science*, 1992, **257**, 219–223.
5. Wirtz, D. and Fermigier, M., One-dimensional patterns and wavelength selection in magnetic fluids. *Phys. Rev. Lett.*, 1994, **72**, 2294–2297.
6. Speliotis, D. E., Magnetic recording beyond the first 100 years. *J. Magn. Magn. Mater.*, 1999, **193**, 29–35.
7. Marshall, C. P. and Dollase, W. A., Cation arrangement in iron–zinc–chromium spinel oxides. *Am. Miner.*, 1984, **69**, 928–936.
8. Satyanarayana, L., Reddy, K. M. and Manorama, S. V., Synthesis of nanocrystalline $Ni_{1-x}Co_xMn_xFe_{2-x}O_4$: a material for liquefied petroleum gas sensing. *Sens. Actuators B*, 2003, **89**, 62–67.
9. Kim, C. S., Kim, W. C., An, S. Y. and Lee, S. W., Structure and Mössbauer studies of Cu-doped Ni–Zn ferrite. *J. Magn. Magn. Mater.*, 2000, **215–216**, 213–216.
10. Peng, C.-H., Hwang, C.-C., Hong, C.-K. and Chen, S.-Y., A self-propagating high-temperature synthesis method for Ni-ferrite powder synthesis. *Mater. Sci. Eng.*, 2004, **B107**, 295–300.
11. Hwang, C.-C., Tsai, J.-S., Huang, T.-H., Peng, C.-H. and Chen, S.-Y., Combustion synthesis of Ni–Zn ferrite powder—influence of oxygen balance value. *J. Sol. St. Chem.*, 2005, **178**, 382–389.
12. Mouallem-Bahout, M., Bertrand, S. and Peña, O., Synthesis and characterization of $Zn_{1-x}Ni_xFe_2O_4$ spinels prepared by a citrate precursor. *J. Sol. St. Chem.*, 2005, **178**, 1080–1086.
13. Zhang, D. E., Zhang, X. J., Ni, X. M., Zheng, H. G. and Yang, D. D., Synthesis and characterization of $NiFe_2O_4$ magnetic nanorods via a PEG-assisted route. *J. Magn. Magn. Mater.*, 2005, **292**, 79–82.
14. Kim, C. S., Yi, Y. S., Park, K.-T., Hae, N. and Lee, J.-G., Growth of ultrafine Co–Mn ferrite and magnetic properties by a sol–gel method. *J. Appl. Phys.*, 1999, **85**, 5223–5225.
15. Liu, C., Zou, B., Rondinone, A. J. and Zhang, Z. J., Reverse micelle synthesis and characterization of superparamagnetic $MnFe_2O_4$ spinel ferrite nanocrystallites. *J. Phys. Chem.*, 2000, **B104**, 1141–1145.
16. Komarneni, S., D'Arrigo, M. C., Leonelli, C., Pellacani, C. and Katsuki, H., Microwave-hydrothermal synthesis of nanophase ferrites. *J. Am. Ceram. Soc.*, 1998, **81**, 3041–3044.

17. Chen, D., Chen, D., Jiao, X., Zhao, Y. and He, M., Hydrothermal synthesis and characterization of octahedral nickel ferrite particles. *Pow. Tech.*, 2003, **133**, 247–250.
18. Upadhyay, C., Mishra, D., Verma, H. C., Anand, S. and Das, R. P., Effect of preparation conditions on formation of nanophase Ni–Zn ferrites through hydrothermal technique. *J. Magn. Magn. Mater.*, 2003, **260**, 188–194.
19. Lee, J.-H., Kim, C.-K., Katoh, S. and Murakami, R., Microwave-hydrothermal versus conventional hydrothermal preparation of Ni- and Zn-ferrite powders. *J. Alloys Comp.*, 2001, **325**, 276–280.
20. Lee, J. H., Maeng, D. Y., Kim, Y. S. and Won, C. W., The characteristics of Ni–Zn ferrite powder prepared by the hydrothermal process. *J. Mater. Sci. Lett.*, 1999, **18**, 1029–1031.
21. Komarneni, S., Fregeau, E., Breval, E. and Roy, R., Hydrothermal preparation of ultrafine ferrites and their sintering. *J. Am. Ceram. Soc.*, 1988, **71**, C-26–C-27.
22. Haberko, K., Bućko, M. M., Haberko, M., Jaśkowski, M. and Pyda, W., Preparation of ceramic micropowders by hydrothermal treatment. In *Vorträge zum Berg- und Hüttenmannischen Tag—Freiberg '87, Herstellen und Charakterisieren feinster Pulver teil II*. Freiberger Forschungshefte, 1988, pp. 71–83.
23. Riman, R. E., Suchanek, W. L. and Lencka, M. M., Hydrothermal crystallization of ceramics. *An. Chim. Sci. Mater.*, 2002, **27**, 15–36.
24. Haberko, K., Characteristics and sintering behaviour of zirconia ultrafine powders. *Ceramurgia Int.*, 1979, **5**, 145–148.
25. Mesing, G. L., Markhoff, C. J. and McCoy, L. G., Characterization of ceramic powder compaction. *Ceram. Bull.*, 1982, **61**, 857–860.
26. Rumpf, H., The strength of granules and agglomerates. In *Agglomeration*, ed. W. A. Knepper. John Wiley & Sons, New York, 1962, pp. 379–418.